High power microwave properties of Zn-Y hexagonal ferrite—parallel pumping size effects

Alexey V. Nazarov, Richard G. Cox, and Carl E. Patton
Department of Physics, Colorado State University, Fort Collins, Colorado 80523

(Received 13 May 2002; accepted for publication 12 July 2002)

The parallel pump spin wave instability threshold field h_{crit} was measured as a function of static field for various size in-plane magnetized thin plates of single crystal Mn substituted Zn-Y at both 9 and 16.7 GHz. The 9 GHz data indicate that (1) the critical modes consist of standing magnetostatic waves and (2) the h_{crit} thresholds depend on the lateral dimensions of the sample. The minimum parallel pumping spin wave linewidths were in the range 3–10 Oe and increased with a decrease in the sample lateral dimensions. These data are consistent with a transit time model and a size limited spin wave linewidth for low wave number critical modes. At 16.7 GHz, thresholds and spin wave linewidths are consistent with the 17.5 GHz and 9.5 GHz ferromagnetic resonance linewidth results and are sample size independent. The data indicate that exchange dominated spin waves are excited for fields below the butterfly curve minimum. These data give a k-dependent spin wave linewidth. The minimum parallel pumping spin wave linewidths were in the range 12–13 Oe. © *2002 American Institute of Physics.* [DOI: 10.1063/1.1505678]

I. INTRODUCTION

High anisotropy hexagonal ferrite materials offer numerous advantages for millimeter wave device applications. Implementation often involves a quantitative understanding of the high power response and the related spin wave linewidth ΔH_k. Recent high power measurements on single crystal c-plane disks of easy plane Zn-Y hexagonal ferrite at 9 GHz gave parallel pump and subsidiary absorption ΔH_k values which were a factor of 2 or more larger than the low power ferromagnetic resonance (FMR) linewidth ΔH_0 and the high power resonance saturation ΔH_k.[1] However, higher frequency parallel pumping data at 16.6 GHz (Ref. 2) and at 36 GHz (Ref. 3) for Zn-Y platelets and spheres give spin wave linewidths which are consistent with FMR results.

The objective of this work was to perform high power ΔH_k measurements and FMR linewidth measurements on Zn-Y single crystal plates at different frequencies for different sizes and shapes, and to use these data to reconcile the linewidth discrepancy noted above. The specific parallel pumping measurements described below were done at 9 and 16.7 GHz on thin rectangular and circular plates. Lateral size, but not thickness, had a significant effect on the 9 GHz ΔH_k values. Larger lateral sizes generally corresponded to smaller spin wave linewidths. The smaller lateral sizes yielded ΔH_k values which were more than half the FMR linewidths. At 16.7 GHz, there were no size effects of significance and the ΔH_k values were about half the 16.7 GHz FMR linewidths and close to the ΔH_0 values at 9 GHz.

These data show that the 9 GHz linewidth inconsistency in Ref. 1 is a sample size effect. At 9 GHz, the critical modes have long wavelengths and relatively low linewidths. These factors combine to produce the size effects found in the data. At 16.7 GHz, the linewidths are generally larger and there are no pronounced size effects. It may be possible to utilize this size effect to increase the high power capability of hexagonal ferrite devices or to develop power limiters for frequencies in the 10 GHz range.

Section II gives the theoretical background for parallel pumping, the critical fields, and ΔH_k. The section also establishes working equations for the data analysis to follow. Section III describes the materials and summarizes the measurement techniques. Section IV presents the experimental results. The interpretation of the 9 GHz data in terms of a size effect and other aspects of the analysis are given in Sec. V.

II. PARALLEL PUMPING IN EASY PLANE FERRITE PLATES

Consider a thin plate single domain ferrite sample with easy plane anisotropy in the plane of the plate. The sample is magnetized to saturation by an external applied uniform static magnetic field **H** in the plane of the plate. A linearly polarized microwave pumping field **h** is applied parallel to **H** and parametric spin waves at a frequency $\omega_k = \omega/2$ are excited above some field-dependent threshold microwave field amplitude h_{crit}. The wave-vector-dependent parallel pump spin wave instability threshold microwave field amplitude for this geometry may be written as[4]

$$h_c(\theta_k, \varphi_k) = \frac{\Delta H_k \omega}{|\gamma||4\pi M_s \sin^2 \theta_k \exp(2i\varphi_k) - H_A|}. \qquad (1)$$

The parameter γ denotes the electron gyromagnetic ratio and $4\pi M_s$ is the saturation induction. The anisotropy field parameter H_A is equal to $2K_u/M_s$, where K_u is the uniaxial anisotropy energy constant. For easy plane anisotropy, as in Zn-Y materials, K_u and H_A are negative. Equation (1) gives h_c for particular spin waves with polar and azimuthal propagation angles θ_k and φ_k defined in a standard right handed (x,y,z) coordinate system with an x axis which is perpen-

 © 2002 American Institute of Physics

Downloaded 28 Oct 2002 to 129.82.31.230. Redistribution subject to AIP license or copyright, see http://ojps.aip.org/japo/japcr.jsp

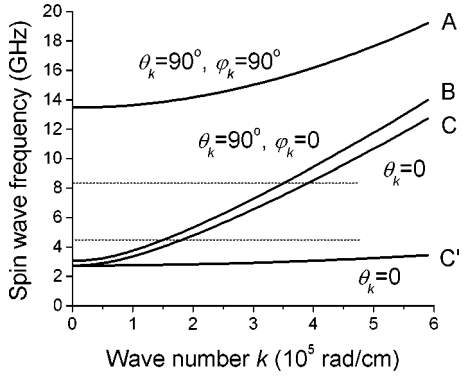

FIG. 1. Schematic bulk spin wave dispersion diagram for a Zn-Y easy plane plate with the static internal in-plane field set to 100 Oe. The graph shows four dispersion curves of spin wave frequency vs wave number k. The angles θ_k and φ_k indicated for each curve designate the polar and azimuthal spin wave propagation angles. The dashed lines correspond to the half frequency spin waves at 4.5 and 8.35 GHz which are excited in the 9 GHz and 16.7 GHz parallel pumping experiments. Curves A, B, and C are for an exchange parameter $D=5\times10^{-9}$ Oe cm^2/rad^2. Curve C′ was calculated for an exchange value $D'=D/50$.

dicular to the plate and a z axis parallel to the in-plane static field **H**. The spin wave linewidth ΔH_k expresses the spin wave relaxation rate.

For a given value of H, one must minimize Eq. (1) relative to all of the available spin waves at $\omega_k=\omega/2$ in order to obtain a theoretical minimum threshold field amplitude $h_{\rm crit}$ for comparison with experiment. The experimental $h_{\rm crit}$ will generally be a function of H. Plots of $h_{\rm crit}$ versus H, usually termed butterfly curves, are an important part of the data presentation and analysis. The minimum measured threshold, in combination with Eq. (1), can be used to determine empirical values of ΔH_k.

As evident from Eq. (1), if the spin wave relaxation rate and corresponding linewidth are independent of the spin wave wave number k and the angles θ_k and φ_k, the critical field $h_{\rm crit}$ will be minimum for $\theta_k=90°$ and $\varphi_k=0$. Note that this spin wave propagation direction is *perpendicular* to the plate. One important implication from the data to follow is that thin plate surface boundary effects can increase the threshold for this type of critical mode and force the wave vector for the excited spin wave in plane.

The range of available spin waves at $\omega_k=\omega/2$ may be defined from the appropriate spin wave dispersion relation for easy plane hexagonal ferrites,[4]

$$(\omega_k/|\gamma|)^2 = [H-4\pi M_s N_z+Dk^2][H-4\pi M_s N_z+Dk^2 - H_A]+4\pi M_s \sin^2\theta_k[H-4\pi M_s N_z+Dk^2 - H_A\sin^2\varphi_k], \quad (2)$$

where D is an exchange parameter and N_z is the demagnetizing factor in the direction of the static field **H**. For a thin plate with **H** in plane, the demagnetizing factor N_z is close to zero. Note that the coordinate system and angles in Ref. 4 are different from the convention here.

Figure 1 shows the principal spin wave dispersion branches from Eq. (2) for the indicated values of θ_k and φ_k and labeled as A, B, C, and C′. The horizontal dashed lines indicate constant frequency cuts at $9/2=4.5$ GHz and $16.7/2=8.35$ GHz. For the dispersion evaluations, γ was set to the free electron value, with $|\gamma|/2\pi=2.8$ GHz/kOe and the internal field $H-4\pi M_s N_z$ was set to 100 Oe. The anisotropy field parameter H_A was set to -9.4 kOe and the saturation induction $4\pi M_s$ was set to 2.33 kG, based on data described in the next section. Reliable values for the exchange parameter D in Zn-Y are scarce. Mita and Shimizu[5,6] cite values of $(7-9)\times10^{-9}$ Oe cm^2/rad^2 for a spin wave propagation direction along the c axis and values about 50 times smaller for propagation in the c plane. Curves A, B, and C were evaluated for $D=5\times10^{-9}$ Oe cm^2/rad^2, the well known value for yttrium iron garnet.[7] The C′ curve was obtained for a 50 times smaller D value and is included to show the effect of the reduced exchange suggested in Refs. 5 and 6. The 4.5 and 8.35 GHz horizontal cuts correspond to half frequency spin waves for the 9 and 16.7 GHz pumping frequencies in the experiment.

The purpose of Fig. 1 is to show the possible critical spin wave modes that may play a role in the parallel pumping experiment. From the above discussion and Eq. (1), one would expect the minimum threshold critical mode to lie on curve B ($\theta_k=90°$ and $\varphi_k=0$) at the appropriate horizontal line frequency cut point. As noted above, however, curve B corresponds to a **k** vector which is perpendicular to the plate plane. If, for some reason, such modes were pushed to a higher threshold, branch C provides an alternative critical mode point for which the wave vector **k** is in plane. Since parallel pumping generally favors half frequency spin waves at $\theta_k=90°$, one might think that a critical mode jump to curve A would be preferred. From Eq. (1), however, one can see that a critical mode point on curve A would have the highest possible threshold.

The above scenario will be changed significantly if there is a reduced exchange for a critical mode **k** vector in the c plane and the plane of the slab. A reduced exchange would bend down curve C, as indicated by the C′ curve. The very large increase in k which would then result from a jump from curve B to C′ would make such a jump highly unlikely.

III. MATERIALS AND EXPERIMENTAL PROCEDURES

The samples for the measurements consisted of thin rectangular and circular plates fabricated from bulk single crystal platelets of zinc Y-Type (Zn-Y) hexagonal ferrite with Mn substitutions. The specific composition was $Ba_2Zn_{1.82}Fe_{11.83}Mn_{0.68}O_{21.2}$.[8] These materials were grown by Dr. M. A. Wittenauer at Purdue University following the same techniques as given in Ref. 9. Zn-Y has easy c-plane magnetocrystalline anisotropy. Six c-plane samples were fabricated. Shapes and dimensions are listed in Table I. The six samples, labeled S1 through S6, are listed in order of decreasing thickness. It was initially expected that the thresholds would be correlated with thickness. It was found, however, that there was more of a threshold correlation with the lateral sample dimensions than with thickness. The microwave data in Table I will be considered shortly.

Downloaded 28 Oct 2002 to 129.82.31.230. Redistribution subject to AIP license or copyright, see http://ojps.aip.org/japo/japcr.jsp

TABLE I. Sample geometry and values of the minimum spin wave instability threshold microwave field amplitude h_{crit}, the minimum spin wave linewidth ΔH_k, and the ferromagnetic resonance linewidth ΔH_0 for the Zn-Y plate samples.

Sample	Shape	Thickness (mm)	In-plane size (mm)	h_{crit} at 16.7 GHz (Oe)	ΔH_k at 8.35 GHz (Oe)	ΔH_0 at 17.5 GHz (Oe)	h_{crit} at 9 GHz (Oe)	ΔH_k at 4.5 GHz (Oe)	ΔH_0 at 9.5 GHz (Oe)
S1	disk	0.34	2.39	6.1	12	18	1.0	2.9	11
S2	disk	0.19	2.32	6.5	12.8	20	0.9	2.6	13
S3	disk	0.14	1.52	6.6	13	20	1.8	5.3	13
S4	disk	0.09	2.32	6.4	12.6	-	1.2	3.5	13
S5	slab	0.09							
	long		1.62	6.6	13	-	2.2	6.4	10
	short		0.72	6.6	13	-	3.5	10.2	-
S6	slab	0.05							
	long		1.44	-	-	15	3.0	8.8	12
	short		0.64	-	-	-	3.5	10.2	-

The static magnetic properties were measured by vibrating sample magnetometry. Magnetization versus applied field was measured on the large disk sample S2 listed in Table I. Data were obtained for applied fields up to 15 kOe, for field directions which were both in plane and perpendicular to the plane of the plate. Shape demagnetizing effects were taken into account empirically, based on the saturation induction determinations and the saturation fields for the in-plane and perpendicular-to-plane field cases. The saturation induction $4\pi M_s$ was determined to be 2.33 ± 0.04 kG, based the magnetic moment values at 15 kG and volume estimates inferred from the sample mass and a theoretical density of 5.48 g/cm^3.[8] Based on this value for $4\pi M_s$ and the measured saturation fields in the parallel and perpendicular configurations, the anisotropy field H_A was determined to be -9.3 ± 0.1 kOe.

Ferromagnetic resonance fields and linewidths were measured for the samples listed in Table I for the in-plane field geometry. All samples were measured at 9.5 GHz. Samples S1, S2, S3, and S6 were also measured at 17.5 GHz. Standard shorted waveguide techniques were used in both cases.[10] The FMR field determinations served as a check on the H_A determinations given above. The average H_A value from these data was -9.4 ± 0.1 kOe. The high power evaluations given below are based on this FMR determination of H_A. The FMR half power linewidths for the measured samples are listed in Table I. These linewidths are 10–13 Oe at 9.5 GHz and 15–20 Oe at 17.5 GHz. As discussed in Ref. 1, typical Zn-Y linewidths from the literature are in this same range. These data will play an important role in the discussion of the spin wave linewidth results to follow.

The high power system that was used for the measurements was similar to that described in Ref. 1. The input microwave pulses were 50 μs wide and the nominal repetition rate was 40 Hz. Peak input powers were in the 1–2 kW range. Separate waveguide setups were used for the 9 and 16.7 GHz data. For 9.0 GHz, a high Q TE_{011} cylindrical cavity was used instead of the rectangular cavity discussed in Ref. 1. This change was done in order to increase the sensitivity and compensate somewhat for the small filling factor. For 16.7 GHz, a standard TE_{102} rectangular cavity was used. For this higher frequency and corresponding smaller cavity, the filling factor was larger and the sensitivity of the rectangular cavity was adequate.

For the 9 GHz high Q cavity measurements, the system was completely automated and operated under computer control based on LABVIEW® software. The system yielded direct data on cavity loss versus microwave field amplitude similar to the results in Fig. 3 of Ref. 1. The experimental h_{crit} results were obtained directly from these computer generated plots. Because of the small filling factors, the nonlinear response was generally quite weak and the accuracy of the h_{crit} determinations was about 15%. Care was taken to make sure that the cavity response at power levels slightly above threshold was not affected by sample heating.

At 16.7 GHz, the larger filling factors made it possible to use a much more rapid and accurate visual determination of the thresholds. In this approach, one simply notes the value of the incident power at the point where the trailing edge of the pulse shows a visible nonlinear response. Due to the larger filling factor, the accuracy of these threshold determinations was significantly higher than those at 9 GHz, and gave h_{crit} values with an error of about 5%. The pulse shape based h_{crit} determination technique and the low Q cavity eliminated any problems with sample heating.

For both frequencies, the measurements were made with the sample in the center of the cavity. The microwave field and the static field were parallel and in the plane of the plate. The corresponding parallel pump geometry matches the setup for the theoretical analysis given in Sec. II. The calibration of the microwave field amplitude at the sample position relative to the incident power was based on microwave perturbation theory and empty cavity parameters as described in Ref. 10. Both the filling factor and the cavity Q affect the accuracy of this calibration.[11] One may estimate the error in the above calibration to be about 10%.

IV. THRESHOLD AND LINEWIDTH DATA

The results of the parallel pumping and FMR measurements are summarized in Table I and Figs. 2 and 3. The table lists minimum h_{crit} values and FMR linewidths for both measurement frequency ranges. The table also gives computed values of the spin wave linewidth ΔH_k from Eq. (1). For

Downloaded 28 Oct 2002 to 129.82.31.230. Redistribution subject to AIP license or copyright, see http://ojps.aip.org/japo/japcr.jsp

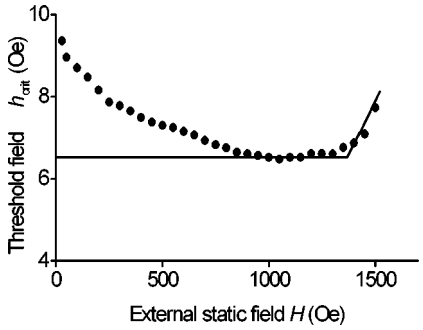

FIG. 2. Parallel pumping threshold h_{crit} as a function of the external static field H for the in-plane magnetized Zn-Y disk S2 with 16.7 GHz microwave excitation. The data and theory are shown by the solid circles and solid line, respectively. The numerical calculations were done for constant spin wave linewidth ΔH_k value of 12.8 Oe.

16.7 GHz, these ΔH_k values correspond to the expected minimum threshold critical modes with $\theta_k = 90°$ and $\varphi_k = 0$, as discussed in Sec. II. For 9 GHz, the listed ΔH_k values correspond to $\theta_k = 0$. This change is related to the size effects noted in the Introduction and discussed in detail below. The results for rectangular samples S5 and S6 are given for fields parallel to the ''long'' and ''short'' sides of the slabs, as indicated. For these samples, the FMR linewidths were obtained for static fields parallel to the ''long'' dimension.

Figures 2 and 3 show data on h_{crit} versus static external field H for 16.7 and 9 GHz, respectively. The solid circles in Fig. 2 show the 16.7 GHz data for sample S2 only. The solid line in the figure shows the theoretical response from Eq. (1) and the minimization procedure described in Sec. II. The spin wave linewidth ΔH_k was set to a constant value of 12.8 Oe, the same as listed in Table I. The demagnetizing factor N_z was set to 0.28 in order to fit the horizontal field response to the data. For this frequency range, all the samples showed a similar response. Curves of h_{crit} versus H are often termed ''butterfly curves.'' Figure 3 shows butterfly curve data at 9 GHz for samples S1 and S5. For S5, data are shown for both the long and the short field directions, as indicated. The S1 data typify the smallest threshold data among all the samples at 9 GHz. No theoretical curves are shown in Fig. 3 because

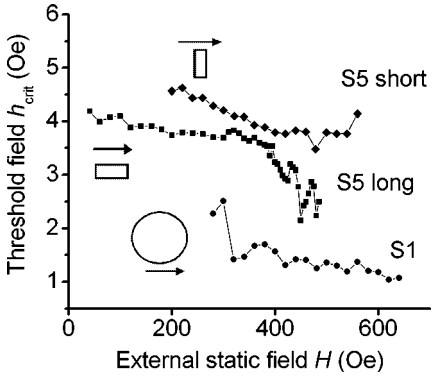

FIG. 3. Data on the parallel pumping spin wave instability threshold h_{crit} as a function of the external static field H for the Zn-Y disk S1 and rectangular plate S5. The static field was in plane and the pumping frequency was 9 GHz. The labels ''S5 long'' and ''S5 short'' indicate the static field orientation along the long and short sides of the rectangular plate, as indicated.

no consistent correlation with the basic theory given above could be found. The implication here, as discussed below, is that size effects dominate the h_{crit} response at 9 GHz.

The key measurement result from Table I concerns the minimum h_{crit} values. At 16.7 GHz, these data show no significant change from sample to sample. At 9 GHz, however, these minimum h_{crit} values show large sample-to-sample changes. Moreover, the main correlation appears to be with the lateral size. A smaller size generally gives a larger threshold. There is no apparent correlation with thickness. Note, for example, that samples S1, S2, and S4 all have about the same lateral size and similar 9 GHz h_{crit} values, even though the thicknesses for these samples vary by a factor of four. Sample S3 has a smaller diameter and a larger threshold. For the rectangular samples S5 and S6, the minimum h_{crit} values also change with the field direction from along the long side to along the short side.

The second important result from Table I concerns connections between the computed spin wave linewidths and the measured FMR linewidths. If one adopts the usual assumption of a linewidth which scales with frequency, one would expect the 8.35 GHz ΔH_k values extracted from the 16.7 GHz minimum h_{crit} data to be close to the 9.5 GHz FMR linewidths. One would also expect the FMR linewidths at 17.5 GHz to be somewhat larger than these values. Both expectations are satisfied by the data in Table I. The 4.5 GHz ΔH_k values extracted from the 9 GHz minimum h_{crit} data are not consistent with this expectation. Some of these linewidths are larger and some are smaller. As noted above, the 9 GHz minimum h_{crit} data vary from sample to sample and appear to be correlated with lateral size.

Overall, the Table I data give (1) 16.7 GHz thresholds and spin wave linewidths which are consistent with the 17.5 GHz and 9.5 GHz linewidth results and are sample independent, and (2) 9 GHz thresholds and spin wave linewidths which vary from sample to sample and show no correlation with the FMR linewidth results. These very different results for the 16.7 and 9 GHz high power data will have important consequences for the size effect discussion of the next section.

Turn now to the figures. The most important result in Fig. 2 is the nearly textbook response found experimentally for parallel pumping at 16.7 GHz. Recall that all the samples had the same response in this frequency range and that the critical modes are at half frequency, or 8.35 GHz. The jump in the data at $H \sim 300$ Oe is attributed to demagnetizing effects. Above this field the sample is saturated and the model calculations can be compared to the data. The measured h_{crit} drops from about 8 Oe at $H = 300$ Oe to about 6.5 Oe at $H = 1000$ Oe and then is approximately constant up to $H \sim 1300$ Oe. There is a distinct kink at $H \sim 1300$ Oe, followed by an increase and truncation at $H \sim 1500$ Oe.

The calculated curve for $\Delta H_k = 12.8$ Oe provides a good match to the data from $H \sim 1000$ Oe up to the truncation point. The kink at $H \sim 1300$ Oe corresponds to the point where the half frequency spin waves are forced to $k = 0$.[12] The increase in the calculated h_{crit} above this kink field point is due to a decrease in the θ_k for the critical modes. The h_{crit} versus field curve then truncates at $H \sim 1500$ Oe as the criti-

Downloaded 28 Oct 2002 to 129.82.31.230. Redistribution subject to AIP license or copyright, see http://ojps.aip.org/japo/japcr.jsp

cal mode goes to $\theta_k = 0$. There are no critical modes available for instability at higher fields. The match up of the theory to the data from the kink point to the truncation field provides proof positive that the critical modes lie on curve B in Fig. 1. Otherwise, there would be no kink in the response. This means that the minimum threshold spin waves below the kink point have $\theta_k = 90°$ and $\varphi_k = 0$ and a **k** which is perpendicular to the static field and the disk plane.

The increase in the measured h_{crit} as the field falls below 1000 Oe may be attributed to an increase in ΔH_k with k for Zn-Y.[3] Such an increase in k is evident from Fig. 1. The point at which the 8.35 GHz dashed line cut crosses the ($\theta_k = 90°$, $\varphi_k = 0$) dispersion branch line (curve B) determines the critical mode k value. This intersection point moves to higher k as the field is decreased and curve B moves down.

As noted, the above data and the fit of the calculated curve to the data constitute a nearly textbook hexagonal ferrite butterfly curve response. These results are in strong contrast with the data for 9 GHz. Figure 3 shows representative 9 GHz results on h_{crit} as a function of H for parallel pumping in the disk sample S1 and the rectangular plate sample S5. The icons and arrows show the relative lateral sizes and field orientations for the samples. Butterfly curve data for the S5 slab are shown for static fields along the long and short sides of the rectangle, as indicated.

The low field limit of the data in each case corresponds to the saturation field for that particular sample. This field is smallest for the rectangle with the field parallel to the long edge, intermediate for the rectangle with the field along the short edge, and largest for the relatively thick disk sample. The jump in h_{crit} below $H \sim 300$ Oe for sample S1 is due to this effect. The ranges of static fields for the data on each sample are all about the same. This confirms the fact that the threshold data are for about the same range of internal fields defined by the critical mode limits discussed above. The S5 data sets truncate at some high field limit as discussed above. The high field limit for S1 was set by the proximity of the magnetostatic mode resonances for fields above about 650 Oe. These particular data were selected to demonstrate the effect of sample size on the thresholds at 9 GHz. As Table I shows, the other samples give minimum h_{crit} values which range between 0.9 and 3.5 Oe, the same range as the data in the figure. As noted in the introduction, a larger lateral size generally corresponds to a lower threshold. The data in Fig. 3 and Table I constitute the proof of this effect.

There is one final experimental point to note from the data in Fig. 3. For sample S5, with H along the long edge of the slab, one can see several distinct dips at the high field end of the butterfly curve. When S5 has the field along the short side, the data appear to show one somewhat less pronounced dip. The presence of these dips, in combination with the overall lateral size correlations for the 9 GHz thresholds, will be the starting point for the discussion below. These results support qualitative and quantitative arguments for critical modes in the 9 GHz measurements which have an in-plane wave vector, rather than the out-of-plane **k** from the theory and the data at 16.7 GHz.

V. DISCUSSION—CRITICAL SIZE EFFECTS

The data in Figs. 2 and 3 and Table I show important contrasts between the high power response in the 9 GHz low frequency and the 16 GHz high frequency ranges. The 16.7 GHz data show (1) an almost textbook h_{crit} versus H response, (2) no significant effect of sample size or thickness, (3) critical modes which match the theory, and (4) a ΔH_k versus k response which matches previous data for Zn-Y. The data and the correlation with theory indicate that the critical modes have wave vectors which are perpendicular to the c-plane plates. In contrast, the 9 GHz data show a strong sample-to-sample variation in the h_{crit} values and the butterfly curve profiles. The thresholds depend on the lateral sample size but not the thickness.

One way to reconcile the lateral sample size dependence for the h_{crit} response at 9 GHz is to make an *ad hoc* assumption that the critical modes have **k** vectors which lie in the plane of the plates, even though the bulk theory gives a minimum threshold for a perpendicular **k** direction. There are two related arguments to support such an assumption. First, the lateral size dependence for h_{crit} suggests that the critical modes lie in plane. Arguments are given below to support this suggestion. Second, the bulk theory gives only a 20% increase in h_{crit} as one moves the critical mode wave vector from perpendicular ($\theta_k = 90°$, $\varphi_k = 0$) to in plane ($\theta_k = 0°$). If there are factors which push the critical mode **k** vector in plane, the effect would not have to be very large to override the bulk prediction.

One can envision a transit time effect to push the critical mode **k** in plane. Transit time models have often been invoked to explain the dependence of h_{crit} on grain size in polycrystalline ferrites.[13–15] The basic idea is that some dimension d in combination with the group velocity v_g of the mode can define a transit time $\tau_d = d/v_g$. If τ_d is less than the intrinsic relaxation time τ_k, then the dimension d limits the lifetime of the mode instead of intrinsic processes. For spin wave instability considerations, one then replaces the intrinsic spin wave linewidth $\Delta H_k = 2/|\gamma|\tau_k$ with a transit time limited linewidth parameter $\Delta H_k = 2/|\gamma|\tau_d = 2v_g/|\gamma|d$.

In the present context, this transit time model can push the critical modes in plane. As listed in Table I, the lateral size L is typically greater than the sample thickness, so that the transit time limited ΔH_k for modes propagating in plane will be smaller. From the data given above, the average threshold follows the relation $\langle h_{\text{crit}} \rangle = C/L$, where C is on the order of 0.3 Oe cm. From Eq. (1) with critical modes on branch C in Fig. 1 with $\theta_k = 0°$, the transit model gives

$$C = \frac{2\omega v_g}{|\gamma|^2 |H_A|}. \tag{3}$$

A match to the empirical C value noted above requires a group velocity on the order of 8×10^6 cm/s. Such group velocities are in the range expected for low k magnetostatic modes in the relatively thick plates used in the current measurements.

Even though the above model offers a plausible argument for in-plane critical modes and sample size dependent

Downloaded 28 Oct 2002 to 129.82.31.230. Redistribution subject to AIP license or copyright, see http://ojps.aip.org/japo/japcr.jsp

thresholds which agree qualitatively with the data, there are still many unresolved problems. Why, for example, do these effects occur at 9 GHz but not at 16.7 GHz? As the threshold data and theoretical comparisons in Fig. 2 show, the 16.7 GHz response matches expectations from the bulk spin wave theory.

A second question closely related to the first concerns the wave numbers for the critical modes. The critical modes for the 16.7 GHz data clearly have wave numbers which range from near zero at the butterfly curve minimum up to values on the order of $(3-4)\times 10^5$ rad/cm at low field. These values, as well as the upturn in threshold as the field is reduced are consistent with the bulk theory as well as the detailed measurements in Ref. 3.

For the transit time arguments to apply at 9 GHz, however, one requires low k modes. The usual high k exchange dominated critical modes which explain the 16.7 GHz data have very low group velocities and scattering lifetimes which are well above the intrinsic spin wave lifetimes. One possible signature for the presence of low k critical modes at 9 GHz is given by the structure in the butterfly curve data in Fig. 3 for the rectangular sample S5. When the field is parallel to the long side, there are three pronounced equidistant dips over the field interval 400–480 Oe and a smaller dip at about 380 Oe. When the field is along the short side, there is a single dip at about 480 Oe. Such structure is the usual signature for low wave number standing mode resonances related to the sample dimensions.[16]

The results in Ref. 16 were for parallel pumping in thin yttrium iron garnet (YIG) films. The standing modes were across the film cross section and related to thickness. Subsidiary absorption butterfly curves for single crystal yttrium iron garnet (YIG) spheres also show a structure for the low k critical modes which looks similar to the response here.[17] For subsidiary absorption in YIG films, Brillouin light scattering measurements have also been used to verify the low k nature of the critical modes.[18] It is important to note that the planar anisotropy in Zn-Y makes it possible to excite critical modes at $\theta_k=0$, while this is not possible in isotropic ferrites. In the present case, the presence of a high mode ellipticity even for $\theta_k=0$ makes it possible to move the minimum threshold critical mode wave vector in plane and produce the effects discussed here.

VI. SUMMARY AND CONCLUSION

Parallel pumping spin wave instability threshold measurements have been made on single crystal in-plane magnetized easy plane plates of Mn substituted Y-type hexagonal ferrite materials at 9 and 16.7 GHz and room temperature. The FMR linewidth measurements were performed at 9.5 and 17.5 GHz. Overall, the data give (1) 16.7 GHz thresholds and spin wave linewidths which are consistent with the 17.5 GHz and 9.5 GHz FMR linewidth results and are sample independent, and (2) 9 GHz thresholds and spin wave linewidths which vary from sample to sample and show no correlation with the FMR linewidth results.

A nearly textbook response is found experimentally for parallel pumping at 16.7 GHz. The data indicate a k-dependent spin wave linewidth with minimum $k=0$ value of 12 Oe. At 9 GHz, the data suggest that the critical modes are pushed in plane and the critical mode wave numbers are low. The sample-size-dependent thresholds can be explained by a transit time model if one assumes low k values and large group velocities for the critical modes.

These experimental and theoretical results raise important questions about the critical modes and spin wave linewidths in hexagonal ferrite materials. First, the origin of the sample-size-dependent thresholds at 9 GHz is not clear. Second, there is the related question of the critical mode properties at both frequencies. The apparent low k values at 9 GHz must relate to magnetostatic mode considerations. The high k modes at 16.7 GHz must relate to high k exchange dominated modes.

Irrespective of these problems, one can conclude that it is possible to control h_{crit} through the sample size at 9 GHz. This effect is due to the empirical fact that the wave vectors are in plane, the k values are low, and lateral size effects control the thresholds. As a part of further work, it will be important to identify the actual wave vectors for the critical modes and determine the nature of the anisotropic exchange and the magnetostatic spin wave spectrum.

ACKNOWLEDGMENTS

This work was supported by the United States Office of Naval Research, Grant No. N00014-94-1-0096. The materials were grown by Dr. Michael A. Wittenauer at Purdue University under ONR Grant No. N00014-91-J-1323. Dr. Jerome J. Green is acknowledged for helpful discussions.

[1] R. G. Cox, C. E. Patton, M. A. Wittenauer, P. Kabos, and L. Chen, J. Appl. Phys. **89**, 4454 (2001).
[2] J. J. Green and B. J. Healy, J. Appl. Phys. **34**, 1285 (1963).
[3] A. G. Gurevich, A. V. Nazarov, O. A. Chivileva, and V. V. Petrov, Phys. Solid State **41**, 1513 (1999).
[4] E. Schlömann, R. I. Joseph, and I. Bady, J. Appl. Phys. **34**, 672 (1963).
[5] M. Mita and H. Shimizu, J. Phys. Soc. Jpn. **35**, 414 (1973).
[6] M. Mita and H. Shimizu, AIP Conf. Proc. **24**, 514 (1975).
[7] A. G. Gurevich and G. A. Melkov, *Magnetic Oscillations and Waves* (CRC Press, Boca Raton, 1996).
[8] M. A. Wittenauer (private communication).
[9] M. A. Wittenauer, J. A. Nyenhuis, A. I. Schindler, H. Sato, F. J. Friedlaender, J. Truedson, R. Karim, and C. E. Patton, J. Cryst. Growth **130**, 533 (1993).
[10] J. J. Green and T. Kohane, SCP Solid State Technol. **7**, 46 (1964).
[11] J. R. Truedson, P. Kabos, K. D. McKinstry, and C. E. Patton, J. Appl. Phys. **76**, 432 (1994).
[12] A. V. Nazarov, C. E. Patton, R. G. Cox, L. Chen, and P. Kabos, J. Magn. Magn. Mater. **248**, 164 (2002).
[13] Q. H. F. Vrehen, H. G. Beljers, and J. G. M. de Lau, IEEE Trans. Magn. **MAG-5**, 617 (1969).
[14] C. E. Patton, J. Appl. Phys. **41**, 1637 (1970).
[15] D. G. Scotter, J. Appl. Phys. **42**, 4088 (1971).
[16] G. Wiese, L. Buxman, P. Kabos, and C. E. Patton, J. Appl. Phys. **75**, 1041 (1994).
[17] C. E. Patton and W. Jantz, J. Appl. Phys. **50**, 7082 (1979).
[18] W. D. Wilber, J. G. Booth, C. E. Patton, G. Srinivasan, and R. W. Cross, J. Appl. Phys. **64**, 5477 (1988).

Downloaded 28 Oct 2002 to 129.82.31.230. Redistribution subject to AIP license or copyright, see http://ojps.aip.org/japo/japcr.jsp